SIMULATING AIRBORNE LINE SCANNER IMAGERY

DOI:10.52113/3/eng/mjet/2013-02-02/83-92

Dr. Rasheed Saleem Abed
Remote Sensing Center
University of Mosul
mosul_5@yahoo.com

A.R.Santhakumar
Emirate Professor
IIT. Madras, Chennai
India

Abstract

Simulation is used to view or evaluate processes that are costly, difficult to perform or time consuming, or simply for educational and display purposes. In photogrammetry, airborne line scanner imagery differs from normal perspective photography in geometric properties. This work introduces the development of a program used for airborne line scanner image simulation. Two products have been discussed, raster image data and ground coverage.

Keywords: Line Scanner, Pushbroom, Simulation, Photogrammetry

محاكاة صورالماسح الجوي الخطي

الخلاصة

تستخدم المحاكاة للتحقق من الأعمال التي يتطلب تنفيذها سعرا مرتفعا او جهدا كبيرا او وقت طويل. او ربما تستخدم لأغراض التعليم والتوضيح. وفي المساحة التصويرية تختلف صور الماسح الجوي الخطي عن التصوير العادي المنظور في بعض الصفات الهندسية. في هذا البحث يتم تطوير برنامج نمذجة صور الماسح الجوي الخطي وفيه تتم مناقشة ناتجين رئيسيين هما الصورة بهيئة الخلايا وكذلك حدود التغطية الأرضية.

الكلمات المرشدة: الماسح الخطي. النمذجة. المساحة التصويرية.

***Received at 3/6/2012** *** Accepted at 25/6/2013**

Introduction

Unlike aerial frame cameras, airborne multispectral scanners offer the possibility for collecting additional spectral data in and beyond the visible range. The collected data is used for improved image understanding and interpretation. Airborne line scanner (or push-broom) images have different geometric characteristics than the case of normal aerial photography [1]. It consists of a semiconductor line (or array) of CCD arranged perpendicular to the direction of flight in the focal plane of a lens. It scans the terrain line by line as in figure 1. Thus the imaging is continuous during flight. During the continuous scan, the collected data are accumulated (with up to hundreds of single-line frames per second) into an image product. This configuration leads to central perspective within scan lines and parallel projection in flight direction. The in-line ground sampling distance (GSD) depends on flight altitude and the CCD configuration. The in-flight GSD is determined by the flight speed and the exposure (integration time) and is usually adapted to be consistent with the in-line GSD; however, under or oversampling is possible due to disturbances. The exterior orientation parameters of the result image can be computed from additional measurements such as joint GPS/IMU processing as described by Sun et al. [2].

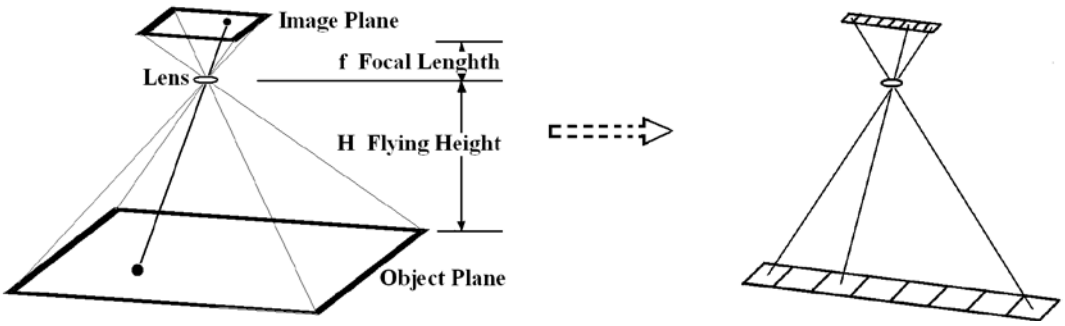

Figure 1. Geometry of normal aerial photography and line scanner CCD analogy.

Collected imagery can have one or more of artifacts such as smearing, blurring.. etc. These effects result from various reasons. The more serious being the effects of atmospheric turbulence on the aircraft during flight. Which may cause change of the roll (wing up or wing down of the aircraft), pitch (nose up or nose down) and yaw angles (deviation from flight line). Or may affect the speed or altitude of the aircraft. Figure 2 shows an example of strong image distortion due to fast roll change [1]. Varying the speed of the aircraft may cause under or over sampling which may affect the GSD value. These effects can cause up to hundreds of meters of errors in coordinates.

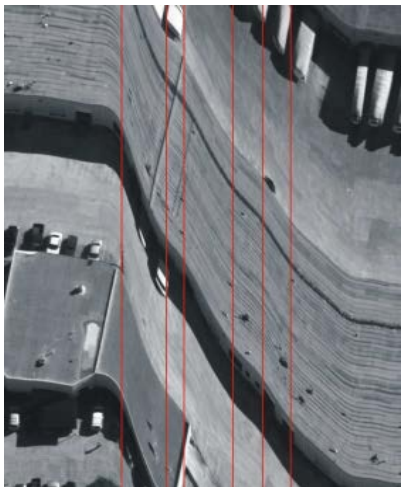

Figure 2. Image of the nadir with strong distortions due to a fast roll move. After [1].

Basic theories in mathematics and algorithms used for photogrammetry have been established in the 20th century. Various literatures present algorithms, formulae and derivations and their use [3],[4],[5],[6],[7].

Many problems in photogrammetry have been studied using simulation techniques. In its analogous form, normal aerial photogrammetry, the oldest and most widely used for mapping, reported uses of simulation to generate fictitious photogrammetric data dates back to 1940s. In the following years, more sets of photographs have been generated with increased complexity for calculating coordinates and other image products.

Before 1960s, hand calculations were used for generating simulated data for many photogrammetric purposes. That was a limiting factor for producing large volume of simulated data. In the present times, computer programs for photogrammetric analysis, solutions and simulation are available. Examples of applications are found in programs such as CRISP, BINGO and STARS [7],[8], which were used for simulation and evaluation of network design.

The geometry of pushbroom scanners have been analyzed in many publications [1],[2],[9],[10]. In airborne line scanners, the continuous imaging of adjacent lines is usually disturbed by instability of the aircraft. The geometry of the image cannot be strictly controlled. McGlones has modeled this effect and used interpolation methods to generate imaging parameters [10].

In this paper the author have identified a need for simulators that deal with the special case of line scanner geometry. This work presents the design of an airborne line scanner image data simulator. A low cost small program package that is easy to use. With interactive capability, the program generates data that is useful for research, visualization and educational purposes.

Mathematics of Line Scanner Images

During platform movement, the terrain is continuously projected onto the sensor one line at a time. In case of simultaneous read-out of all line elements during each time interval, the image of each line of detectors is separately treated as a central perspective. i.e. as a digital frame camera having only one raw of pixels as shown in figure 1.

Image coordinates (x,y) can be calculated from local coordinates of ground points according to the following equation 1 [6]. which is explained also in figure 3.

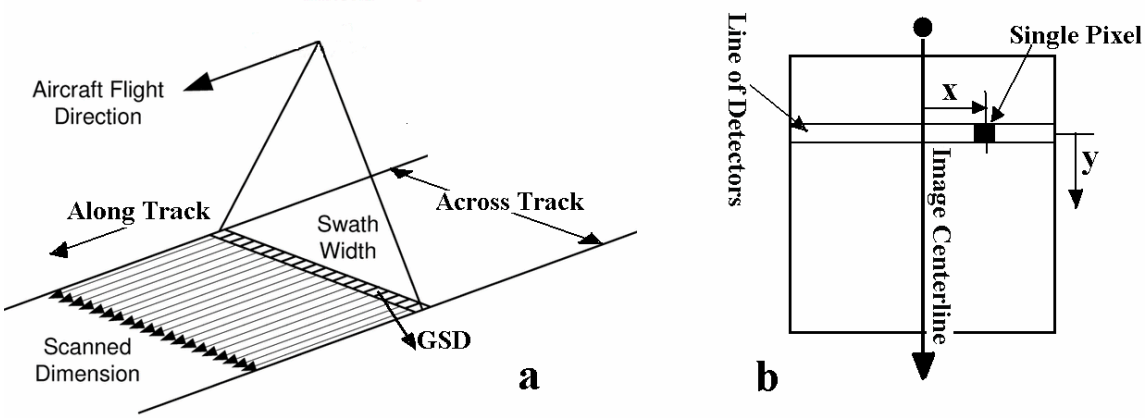

Figure 3. Geometry of a) scanning process, and b) image coordinate system.

$$x = x_o - f \left\{ \frac{(r11\ Xp + r12\ Yp + r13\ Zp)}{(r31\ Xp + r32\ Yp + r33\ Zp)} \right\} \qquad (1)$$

y =coordinates perpendicular to the detector array.
x =the column distance to the image center scaled to the detector spacing.
f = lens focal length in mm.
$[Xp, Yp, Zp]^T$ = Vector of differences in local vertical coordinate system between camera and ground stations.
r = Orthogonal rotation matrix expressing image exposure station, defined as follows..

$r1_i = [\cos\phi \cos\kappa, \sin\omega \sin\phi \cos\kappa + \cos\omega \sin\kappa, -\cos\omega \sin\phi \cos\kappa + \sin\omega \sin\kappa]$
$r2_i = [-\cos\phi \sin\kappa, -\sin\omega \sin\phi \sin\kappa + \cos\omega \cos\kappa, \cos\omega \sin\phi \sin\kappa + \sin\omega \cos\kappa]$
$r3_i = [\sin\phi, -\sin\omega \cos\phi, \cos\omega \cos\phi]$

Here, ω, ϕ, κ are rotations around X,Y,Z axis, i =1,3.

Resolution of aerial photographs or (digital camera systems and line scanners) expresses the ability to resolve ground features. It is also defined as the side length of single pixel in mm. In line scanner (pushbroom) geometry, equations 2, 3 and 4 are used in combinations.

$$R = \frac{\text{(image width or height in mm)}}{\text{(Number of pixels)}} \qquad (2)$$

Where, R is the image pixel resolution in mm in the specified direction (square pixels).
The nominal ground resolution Rg (m) is, [11].

$$Rg = \frac{R}{\text{image scale} \cdot 1000} \text{ or } = \frac{R.\ f}{H} \qquad (3)$$

Where
H = Camera or sensor height above ground in meters.

f = Camera focal length in mm.

However, for line scanners, the ground resolution along flight line there are two kinds of resolution as defined below,

i) Nominal ground resolution, Rg (m) (Similar to Equation (3)).

ii) Actual ground resolution, Ra. (m). (affected by the speed of the aircraft and sensor integration time.)

$$Ra = t \cdot v \quad (4)$$

Where,

t = sensor integration time in sec.

v = aircraft speed. m/sec.

The surface reflectance values at a specified location expressed as digital numbers DNs, f(x, y) are calculated by bilinear interpolation from the values at the surrounding four corner locations. This method is convenient for gridded sample files as usually the case in digital elevation models DEMs and for DN values that are extracted from existing ortho products.

The interpolation equation used is.

$$f(x, y) = a + b \cdot x + c \cdot y + d \cdot x \cdot y \quad (5)$$

Where x, y is the location of the required value within the grid cell.

f(x, y) = the required interpolated DN value.

a, b, c, d = bilinear interpolation parameters to be calculated from the four surrounding cell corners.

Raster image simulation deals with ground cell heights in the form of DEM values and the corresponding gray values for the imaged area. The line scanner here is treated as a digital aerial camera having only one CCD line perpendicular to the flight direction. For each instance of imaging, the sensor location and attitudes have to be defined.

According to the image format, length, width in millimeters and number of rows and columns being specified, the pixel resolution is calculated in both directions. After addressing the X and Y ground location of the specified image pixel, the value of reflectance in the form of DN is calculated. The generated matrix of reflectance values (DN) is saved on the disk in a suitable image file format.

For calculating ground track positions and projected image boundaries of the line scanner image, the four corners of each single scan line image are projected on the ground. Consecutive lines along flight direction form the full image. To calculate image locations of any provided ground control points (GCPs), these are examined to check whether they fall within the range of the present scanning frame. Image coordinates are then calculated relative to the whole frame.

Production of Simulated Photographs

The program have been written using the C language which have efficient capability to deal with images and use pointer addressing to increase processing speed.

DEM and related DN data files were prepared for testing this program. A subset was extracted from the output of a previous digital photogrammetric work [8]. A rectangular portion of an area

of 140 X 300 m is extracted. The elevation data of the selected area was prepared in a regular grid of points. The chosen grid size is 1 m. to match the DN spacing interval provided by the original orthoimage. The imaged area resembles clear bright lines of roads and few agriculture fields with sparse trees. The selected area has an elevation range of 299 to 322 m. Figure 4(a, b, c) shows image and elevation data of the test area used in this study.

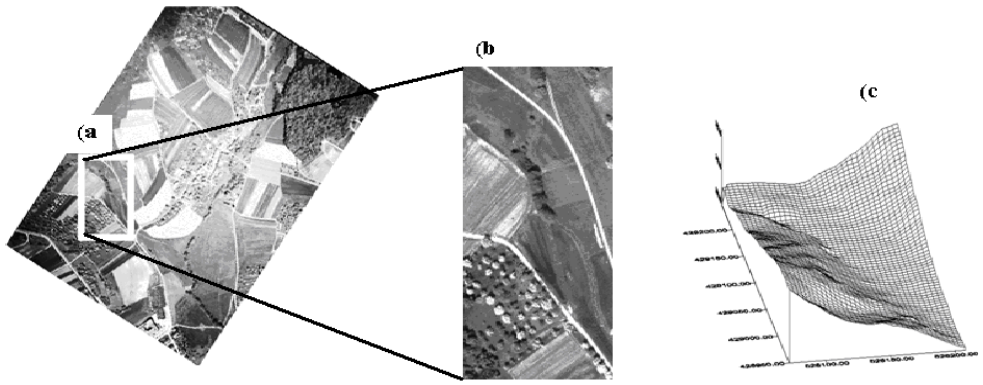

Figure 4. sample image and corresponding elevation data used in this work.

Various cases of simulations have been produced for airborne line scanners and shown in Figures 5(a) through (c). Figure 5(a) shows the result of ideal imaging along the centerline of the area at constant flight elevation of 550m. The relief effects in this case are seen at the image corners. Figure 5(b) shows scanning at a height of 800m. An obvious reduction in the crosswise image scale is seen. The output of the nadir imaging while moving on a flight line exactly vertically above the left side of the area is shown in Figure 5(c). Relief distortion is seen along the right bounding line of the image. No relief distortion is created along the nadir line. Figure 6(a) demonstrates the gradual increase in scanner height during the scanning run. The effect can be perceived in the gradual change of image scale while the height is increasing.

Introducing sinusoidal oscillation to the scanner in the roll angle (ϕ) during motion is demonstrated in figure 6(b). The deformed road line is clearly seen. The result of scanning in forward looking angle (pitch of $30^{o)}$ is demonstrated in figure 6(c). In this case, the initial part of the area is obscured due to the specified inclined direction of imaging.

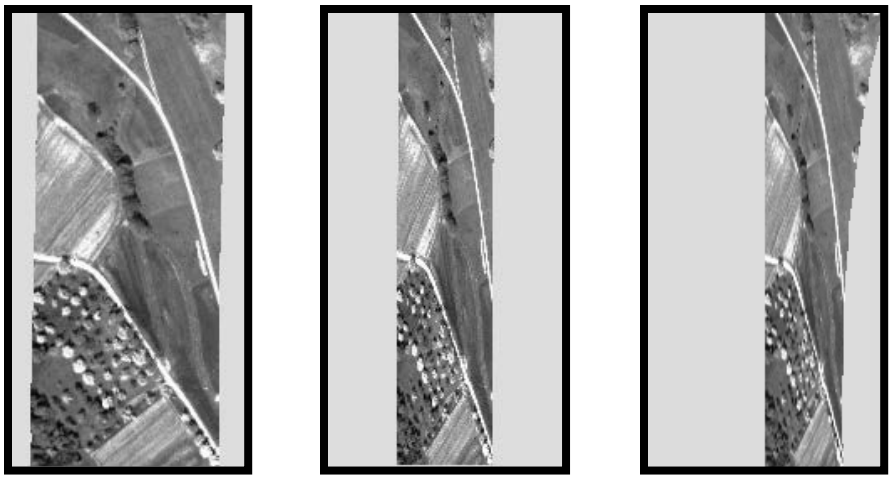

(a) (b) (c)

Figure 5. A set of simulated line scanner images produced with steady system parameters. (a) Scanning vertically along the centerline of the area. (b) At higher altitude. (c) Along the left side of the area

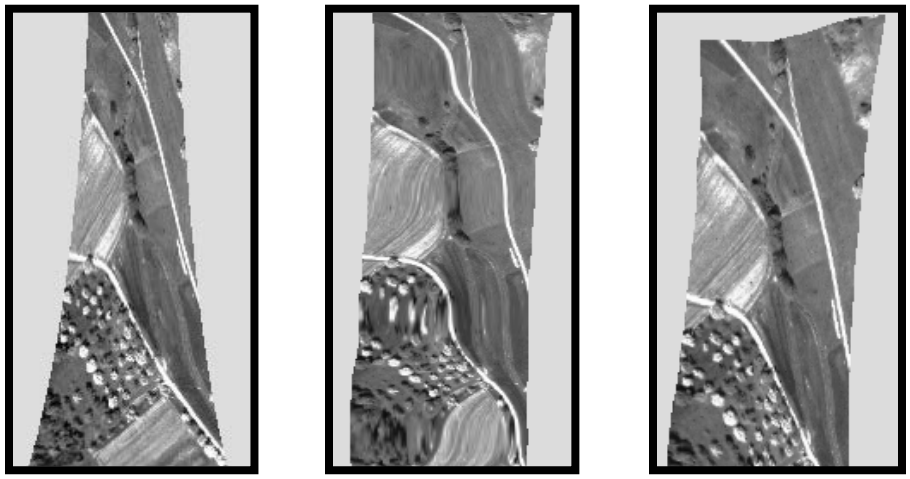

(a) (b) (c)

Figure 6. (a) Scanning at variable (increasing) altitude. (b) Simulated sensor oscillation in the ϕ scan angle, (c) Scanning at forward looking pitch angle of 30^{o}

Production of Simulated Ground Track Coverage

The average terrain height is used as the basic flat surface upon which image projections are drawn. Imaged boundary lines and sensor tracks can be visualized. Figures 7 through 9 show sample displays of airborne line scanner ground-track coverage. Projected image limits are shown as well as the nadir line of the scanner during motion. The GCPs as provided by the user are shown in the display. Figure 7 demonstrates scanning at azimuth angle of 339° in ideal conditions of aircraft motion. The effect of gradual increase in the flying height to 1000 m and using 150.0mm lens is shown in figure 8. It shows the across-track widening of the covered terrain. The effect of sinusoidal oscillation of the scanner with oscillating roll (ϕ) angle value is shown in Figure 9.

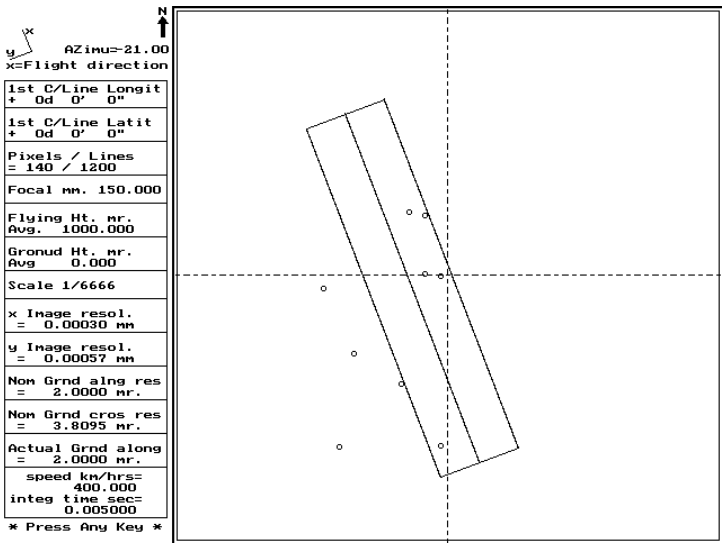

Figure 7. Ground track of ideal scanning at azimuth of 339˚ (-21˚)

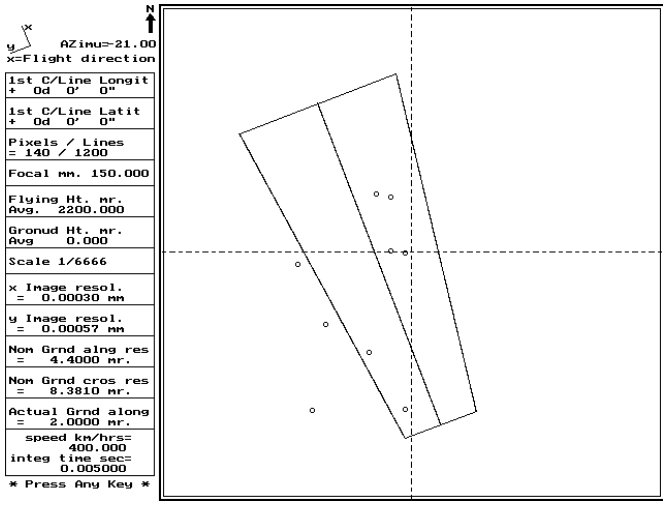

Figure 8. Ground track at linear variation in scanner height

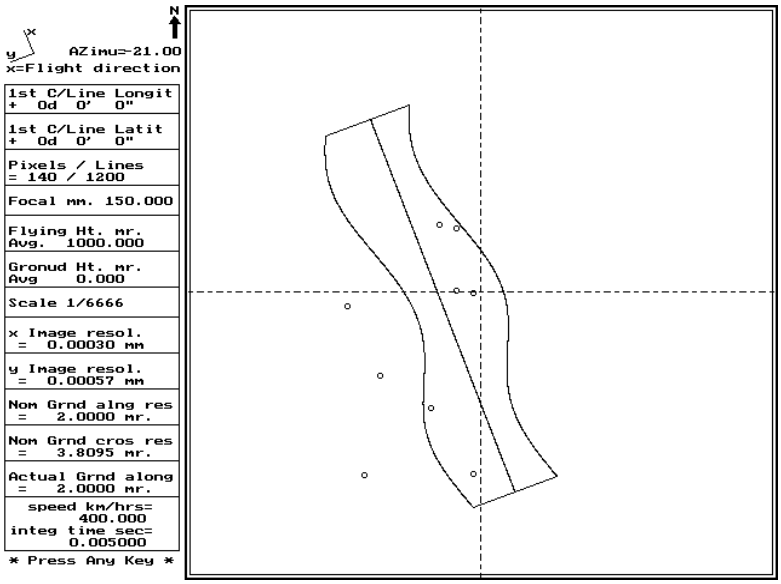

Figure 9. Scanning with oscillating roll angle (ϕ).

Program Performance

In raster image calculations, a major factor in performance is the computation time that depends mainly on the number of pixels in the digital photograph and the amount and kind of calculations involved and variability of points heights. At higher elevations of ground points (or lower sensor height), the program requires more time for calculations due to the iterative solution. The speed is also slower for ground points located off the nadir line. Table 1 compares an ordinary full frame digital aerial image with line-scanner image having the same number of pixels (the example case of figure 4). Varying heights are tested. Also a vertical and oblique cases. It shows computational times in seconds of simulation runs. For Line scanner processing, the program starts new calculations for each imaging instance.

Table 1 Execution times in seconds for varying cases of raster image simulation.

Sensor position And direction	1000 meters height		400 meters height	
	Vertical	Oblique	Vertical	Oblique
Aerial image	1.648	1.648	7.857	7.362
Line Scanner	11.264	11.318	14.065	14.125

Conclusions

The example implementations of the program that were negotiated show that benefits from a user point of view can support a researcher in providing forms of accurate data for a specific problem. It also supports a trainee and student through providing a program that presents a module of

multiple uses. The practice of this program can be increased to involve several other techniques in photogrammetry.

References

1. Gehrke, S. and R. Uebbing. (2011)."QUANTIFICATION OF TURBULENCE FOR AIRBORNE LINE-SCANNER IMAGES". ASPRS Annual Conference. Milwaukee, Wisconsin. May 1-5.
2. Sun, H., Morin K., et al. (2006)'IPAS – Leica Geosystems' High Accuracy GPS/IMU Integrated System for Air- borne Digital Sensors". Proceedings ASPRS Annual Conference. Reno, N
3. Doyle F. J. (1966) 'Fictitious Data Generator for Analytical Aerotriangulation', Photogrammetria, 21, pp. 179-194.
4. Thompson M. M. (Ed.) (1966) 'Manual of Photogrammetry', American Society for Photogrammetry, Vol. 1., 536 pages.
5. Unruh J. E. (1980) 'Digital Image Simulation for Photogrammetric Applications', Ph.D. Thesis, Purdue University.
6. Wolf R. P. (1972) 'Elements of Photogrammetry', McGraw-Hill, 500 pages.
7. Karara H.M. (Ed.) (1989) 'Non-Topographic Photogrammetry', ASPRS, 444 pages.
8. Rasheed S. and A. R. Santhakumar (2001) 'An Object-Oriented Program for Photogrammetric Data Simulation', Proceedings, ICORG- Hyderabad, India Vol. 1., pp. 375-379.
9. Jama, M, et al. (2010). 'Analyzing Scene Geometries for Stereo Pushbroom Imagery'. Proceedings ASPRS Annual Conference. San Diego, California. April 26-30
10. McGlone C. and Mikhail E.M. (1985) 'Evaluation of Aircraft MSS Analytical Block Adjustment', Photogrammetric Engineering and Remote Sensing, Vol. 51., No. 2, pp. 217-225.
11. Sabins, F. (1996)."Remote Sensing : Principles and Interpretation". 3rd edition. W H Freeman & Co.